

## Precision Determination of $r_0\Lambda_{\overline{\text{MS}}}$ from the QCD Static Energy

Nora Brambilla,<sup>1</sup> Xavier Garcia i Tormo,<sup>2</sup> Joan Soto,<sup>3</sup> and Antonio Vairo<sup>1</sup>

<sup>1</sup>*Physik Department, Technische Universität München, D-85748 Garching, Germany*

<sup>2</sup>*Department of Physics, University of Alberta, Edmonton, Alberta, Canada T6G 2G7*

<sup>3</sup>*Departament d'Estructura i Constituents de la Matèria and Institut de Ciències del Cosmos, Universitat de Barcelona, Diagonal 647, E-08028 Barcelona, Catalonia, Spain*

(Received 15 June 2010; published 15 November 2010)

We use the recently obtained theoretical expression for the complete QCD static energy at next-to-next-to-next-to leading-logarithmic accuracy to determine  $r_0\Lambda_{\overline{\text{MS}}}$  by comparison with available lattice data, where  $r_0$  is the lattice scale and  $\Lambda_{\overline{\text{MS}}}$  is the QCD scale. We obtain  $r_0\Lambda_{\overline{\text{MS}}} = 0.622^{+0.019}_{-0.015}$  for the zero-flavor case. The procedure we describe can be directly used to obtain  $r_0\Lambda_{\overline{\text{MS}}}$  in the unquenched case, when unquenched lattice data for the static energy at short distances becomes available. Using the value of the strong coupling  $\alpha_s$  as an input, the unquenched result would provide a determination of the lattice scale  $r_0$ .

DOI: 10.1103/PhysRevLett.105.212001

PACS numbers: 12.38.Aw, 12.38.Bx, 12.38.Cy, 12.38.Gc

The energy between a static quark and a static antiquark is a fundamental object to understand the behavior of quantum chromodynamics (QCD) [1]. Its long-distance part encodes the confining dynamics of the theory while the short-distance part can be calculated to high accuracy using perturbative techniques. Perturbative computations of the short-distance part have been performed for many years [2,3] and the two-loop corrections have been known for quite some time now [4–6]. When using perturbation theory to calculate the short-distance part, the virtual emission of gluons that can change the color state of the quark-antiquark pair (so-called ultrasoft gluons) produce infrared divergences, which induce logarithmic terms,  $\ln\alpha_s(1/r)$ , in the static energy. Those effects, which first appear at the three-loop order, were identified in Ref. [7] and calculated in Refs. [8,9] using an effective field theory framework [10,11]. That framework also allows for resummation of the ultrasoft logarithms [12], which may be large at small distances  $r$ . Very recently, the complete three-loop corrections to the static energy have become available [13–15]. Combining the results of those calculations with the resummation of the ultrasoft logarithms at subleading order [16,17], the static energy at next-to-next-to-next-to leading-logarithmic ( $\text{N}^3\text{LL}$ ) accuracy, i.e., including terms up to order  $\alpha_s^{4+n}\ln^n\alpha_s$  with  $n \geq 0$ , is now completely known.

In the first part of the Letter, we compare the static energy at  $\text{N}^3\text{LL}$  accuracy with lattice data. The comparison shows that, after subtracting the leading renormalon singularity, perturbation theory reproduces very accurately the lattice data at short distances, thus confirming at an unprecedented precision level the conclusions reached in previous analyses [16,18,19]. In the second part of the letter, the excellent agreement of perturbation theory with lattice data allows us to obtain a precise determination of the quantity  $r_0\Lambda_{\overline{\text{MS}}}$ , where  $r_0$  is the lattice scale and  $\Lambda_{\overline{\text{MS}}}$  is

the QCD scale (in the  $\overline{\text{MS}}$  scheme), a key ingredient to relate low energy hadronic physics with high energy collider phenomenology. This constitutes the main result of our work.

The static energy  $E_0(r)$  at short distances can be written as

$$E_0(r) = V_s + \Lambda_s + \delta_{\text{US}}, \quad (1)$$

where  $V_s$  and  $\Lambda_s$  are matching coefficients in potential Non-Relativistic QCD (pNRQCD) [11] and  $\delta_{\text{US}}$  contains the contributions from ultrasoft gluons.  $V_s$  corresponds to the static potential and  $\Lambda_s$  inherits the residual mass term from the heavy quark effective theory Lagrangian. In order to obtain a rapidly converging perturbative series for the static potential in the short-distance regime, it has been argued that it is necessary to implement a scheme that cancels the leading renormalon singularity [20]. The use of any such scheme introduces an additional dimensional scale (which we call  $\rho$ ), upon which all the quantities in Eq. (1) depend. We will employ the so-called RS scheme [21], in the same way as it was done in Ref. [16]. The explicit expressions for  $E_0$  at  $\text{N}^3\text{LL}$  accuracy were presented in Ref. [16] and will not be repeated here. We refer to that paper for details. The only new ingredient is that the three-loop gluonic contribution to the static potential is now known. At three-loop order the static potential presents infrared divergences, which cancel in the physical observable  $E_0$  after the inclusion of the ultrasoft effects. Therefore, it is necessary to consistently use the same scheme to factorize the ultrasoft contributions for all the terms in Eq. (1). That way one obtains the correct three-loop coefficient for the static energy  $E_0$ , which is independent of the scheme used to factorize the ultrasoft contributions. Refs. [14,15] present the result for the purely gluonic three-loop coefficient of the static potential in momentum space, which we call  $a_3^{(0)}$  (following the

notation of Ref. [15]). We emphasize again that  $a_3^{(0)}$  is scheme dependent. The corresponding coefficient in the static energy can be obtained by taking the  $d$ -dimensional Fourier transform of the momentum-space potential (as calculated in Refs. [14,15]) and adding to it the ultrasoft contribution. In the factorization scheme used in Refs. [14,15], the ultrasoft contribution is given by Eq. (8) of Ref. [14] (which we confirm). Note that the scheme used in Refs. [14,15] is different from the one used in Ref. [16]. If we then subtract Eq. (34) of Ref. [16] (the ultrasoft contribution in the scheme of that paper) from the static energy we get the three-loop gluonic contribution to the static potential in the scheme of Ref. [16] (which we will denote as  $a_{3\text{Ref.}[16]}^{(0)}$ ). By doing that we obtain [15]  $c_0 := a_{3\text{Ref.}[16]}^{(0)}/4^3 = 222.703$ . This was the only missing ingredient of the static energy at  $N^3\text{LL}$  accuracy at the time Ref. [16] was written. Note that the value of  $c_0$  above is within the range (215, 350) predicted in Ref. [16], and considerably lower than the Padé estimate  $c_0 = 313$  commonly used in the literature [22].

We now compare the perturbative results for the static energy with the  $n_f = 0$  lattice data of Ref. [23]. All results are presented in units of  $r_0$ . As it is explained in Ref. [16], an appropriate quantity to plot for this comparison is

$$E_0(r) - E_0(r_{\min}) + E_0^{\text{latt}}(r_{\min}), \quad (2)$$

where  $r_{\min}$  is the shortest distance at which lattice data is available and  $r_0 E_0^{\text{latt}}(r_{\min}) = -1.676$  [23]. Now that the three-loop static potential is known the normalization of the  $u = 1/2$  renormalon singularity  $R_s$ , which is necessary to implement the RS scheme, can be determined using one order more in the perturbative expansion of the potential. We obtain

$$R_s = -1.333 + 0.499 - 0.338 - 0.033 = -1.205, \quad (3)$$

which is the value we will use. The rest of the scales and parameters are set as in Ref. [16]. We note that, in particular, this means that we have  $\rho = 3.25r_0^{-1}$  and  $r_0\Lambda_{\overline{\text{MS}}} = 0.602$  [24]. The comparison of the static energy with lattice data is presented in Fig. 1(a). We recall that all the curves coincide with the lattice point at  $r = r_{\min}$  by construction [as one can see from Eq. (2)]. We note that, due to the singlet-octet mixing in the renormalization group equation for  $\Lambda_s$  (at order  $r^2$  in the multipole expansion of pNRQCD), the  $N^3\text{LL}$  curve (solid black) depends on a constant, which we call  $K_2$ . Power counting tells us that  $|K_2| \sim \Lambda_{\overline{\text{MS}}}$ , but the constant is otherwise arbitrary. We fix it by a fit to the lattice data, which delivers  $r_0 K_2 = -1.98$ . The bands in Fig. 1(a) illustrate the effect of variations in  $r_0\Lambda_{\overline{\text{MS}}} = 0.602 \pm 0.048$  [24] (yellow lighter band) and the effect of adding the term  $\pm C_F \alpha_s^5/r$ , which is representative of the neglected higher-order corrections (green darker band); the remaining parameters are kept at their original values to obtain the bands. The figure confirms that perturbation theory (in the RS scheme) reproduces very

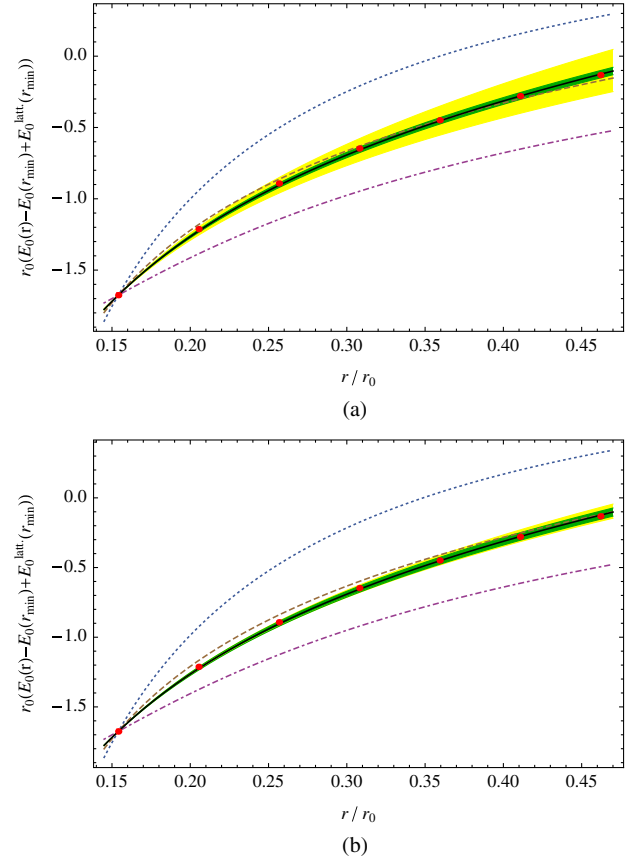


FIG. 1 (color online). (a) Comparison of the singlet static energy with lattice data. We plot  $r_0(E_0(r) - E_0(r_{\min}) + E_0^{\text{latt}}(r_{\min}))$  as a function of  $r/r_0$  and the lattice data of Ref. [23] (red points). The dotted blue curve is at tree level, the dot-dashed magenta curve is at one loop, the dashed brown curve is at two loop plus leading ultrasoft logarithmic resummation and the solid black curve is at three loop plus next-to-leading ultrasoft logarithmic resummation. The yellow (lighter) band is obtained by varying  $r_0\Lambda_{\overline{\text{MS}}}$  according to  $r_0\Lambda_{\overline{\text{MS}}} = 0.602 \pm 0.048$  [24] and the green (darker) band is obtained by adding the term  $\pm C_F \alpha_s^5/r$ , for the solid black curve. (b) Same but using  $r_0\Lambda_{\overline{\text{MS}}} = 0.622^{+0.019}_{-0.015}$  (see text).

well the lattice data for the static energy at short distances. We also note that the band due to the neglected higher-order terms is smaller than the one due to the uncertainty in  $r_0\Lambda_{\overline{\text{MS}}}$ . Those facts indicate that we should be able to use the lattice data to obtain a more precise determination of  $r_0\Lambda_{\overline{\text{MS}}}$ , as we describe later. It is worth emphasizing that the aim of Fig. 1 is to compare with lattice data for the specific  $r$  range displayed in the figure and to see if the theoretical curves follow the lattice data points starting from the point at the shortest distance. The scale  $\rho$  was set to the fixed value  $3.25r_0^{-1}$ , which is at the center of the range, and it was kept the same for all curves. Moreover, the static energy was expressed as a series in  $\alpha_s(\rho)$ , rather than  $\alpha_s(1/r)$ , to reduce the uncertainty associated with  $R_s$  and the specific implementation of the renormalon subtraction.

We will now assume that perturbation theory by itself (after canceling the leading renormalon) is indeed enough to accurately describe the lattice data for the range of  $r$  we are considering, i.e.,  $0.15r_0 \leq r < 0.5r_0$ . That is, we are assuming that nonperturbative effects are small and can be totally neglected. (The leading genuine nonperturbative contribution, which is proportional to the gluon condensate, is of order  $\Lambda_{\overline{\text{MS}}}^4 r^3 / \alpha_s(1/r)$ , and hence parametrically suppressed according to the counting of Ref. [16], which assumes  $\Lambda_{\overline{\text{MS}}} \sim \alpha_s^2/r$ .) With this assumption, we can use the lattice data for the static energy to determine  $r_0\Lambda_{\overline{\text{MS}}}$ . We initially consider the set of  $r_0\Lambda_{\overline{\text{MS}}}$  for which: (i) the perturbative series for the static energy appears to converge, and (ii) the agreement with lattice is improved when increasing the perturbative order of the calculation. If we implement the condition (ii) by demanding that the reduced  $\chi^2$  of the curves decreases when we increase the perturbative order of the calculation, we obtain the range (0.59, 0.7) for  $r_0\Lambda_{\overline{\text{MS}}}$ . We now proceed to improve the precision of that determination. First, we recall that the use of the RS scheme introduced the scale  $\rho$  in the expressions for the static energy. We have used the value  $\rho = 3.25r_0^{-1}$  because it corresponds to the inverse of the central value of the  $r$  range we are comparing with lattice data. That way we keep  $\ln r\rho$  terms from becoming large [16], but in principle any  $\rho$  around that value is valid. We will exploit this freedom to find a set of  $\rho$  values which are “optimal” for the determination of the parameter  $r_0\Lambda_{\overline{\text{MS}}}$  by following the procedure we describe next: (1) We vary  $\rho$  by  $\pm 25\%$  around  $\rho = 3.25r_0^{-1}$ , i.e., from  $\rho = 2.44$  to  $\rho = 4.06$ . (We have used steps of  $1.6 \times 10^{-3}r_0^{-1}$  to do that.) (2) For each value of  $\rho$  and at each order in the perturbative expansion of the static energy, we perform a fit to the lattice data. The parameters of the fit are  $r_0\Lambda_{\overline{\text{MS}}}$  for the curves from tree level to next-to-next-to-leading-logarithmic ( $N^2\text{LL}$ ) accuracy (1-parameter fits), and  $r_0\Lambda_{\overline{\text{MS}}}$  and  $r_0K_2$  for the curve at  $N^3\text{LL}$  accuracy (2-parameter fit). (3) We select those  $\rho$  values for which the reduced  $\chi^2$  of the fits decreases when increasing the order of the perturbative expansion. (4) Finally, from the set of  $\rho$  values obtained above, we select the ones for which the fitted value of  $K_2$  is compatible with the power counting (we require  $|r_0K_2| \leq 2$  [16]). The above steps provide us with a certain range of  $\rho$ . We then consider the set of fitted values of  $r_0\Lambda_{\overline{\text{MS}}}$  at  $N^3\text{LL}$  accuracy (denoted as  $x_i$  below) for that range. In order to give more significance to the better fits, we assign a weight to each of the  $x_i$ . We choose those weights to be given by the inverse of the reduced  $\chi^2$  of the fit. We take the weighted average of the  $x_i$  as our central value for the determination of  $r_0\Lambda_{\overline{\text{MS}}}$  and obtain

$$\bar{x} := \sum_i w_i x_i = 0.622, \quad (4)$$

where  $w_i := \tilde{w}_i / (\sum_j \tilde{w}_j)$  and  $\tilde{w}_i$  is the weight of the point  $x_i$ . To estimate the error that we should associate to that number, we first consider the weighted standard deviation

of that set of values and assign it as an error to the weighted average (a similarly motivated procedure to estimate theoretical errors has been used, for example, in Ref. [25]), we obtain

$$\sigma := \sqrt{\frac{1}{1 - \sum_j w_j^2} \sum_i w_i (x_i - \bar{x})^2} = 0.009. \quad (5)$$

Figure 2 shows the obtained fit values of  $r_0\Lambda_{\overline{\text{MS}}}$  at  $N^3\text{LL}$  accuracy and at  $N^2\text{LL}$  accuracy, for the different values of  $\rho$ . The size of each point in the plot is proportional to its weight. Additionally, we also consider the difference between the weighted averages computed using the  $N^3\text{LL}$  result and the  $N^2\text{LL}$  result and assign it as a second error to the weighted average at  $N^3\text{LL}$  accuracy (we compute the weighted average at  $N^2\text{LL}$  accuracy in the  $\rho$  range obtained after step 3 of the procedure described above, since step 4 applies only to the  $N^3\text{LL}$  result). The value of that difference is 0.003. We sum those two errors linearly and obtain  $0.622 \pm 0.012$ . We present in Table I the obtained values for  $r_0\Lambda_{\overline{\text{MS}}}$  following this procedure at different orders of accuracy. We emphasize that the error assigned to the result must account for the uncertainties associated to the neglected higher-order terms in the perturbative expansion of the static energy; in that sense, we note that Table I shows that our errors at a certain perturbative order always include the central value at the next order, which gives us confidence in the reliability of the procedure. In order to further assess the systematic errors stemming from our procedure, we have redone the analysis using two additional weight assignments: (i)  $p$ -value weights, this analysis gives  $r_0\Lambda_{\overline{\text{MS}}} = 0.632 \pm 0.009$ , and (ii) constant weights, this analysis gives  $r_0\Lambda_{\overline{\text{MS}}} = 0.618 \pm 0.011$ . These two numbers are compatible with our previous value. In our final result, we will quote an error that covers the whole range spanned by the three analyses, which we consider a fairly conservative

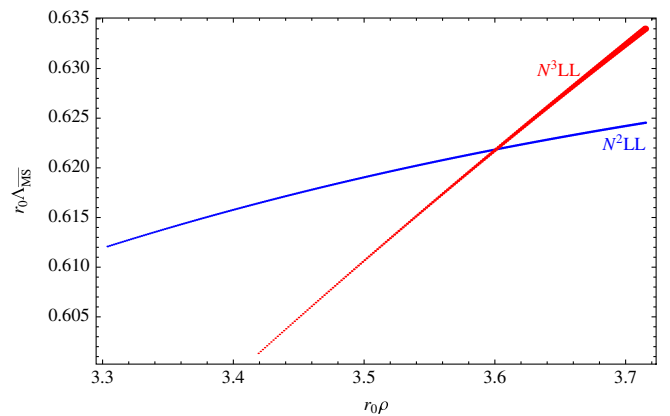


FIG. 2 (color online). Fit values of  $r_0\Lambda_{\overline{\text{MS}}}$  for different values of  $\rho$ . The range of  $\rho$  displayed in the plot corresponds to that obtained after step (3) ( $N^3\text{LL}$  points) or step (4) ( $N^3\text{LL}$  points) of the procedure described in the text. The size of each point is proportional to its assigned weight.



TABLE I. Values of  $r_0\Lambda_{\overline{\text{MS}}}$  obtained at different levels of accuracy. N<sup>3</sup>LL (no PCC) stands for N<sup>3</sup>LL accuracy without imposing the power counting constraint on  $K_2$ , i.e., omitting step (4) in the procedure described in the text. The first error corresponds to the weighted standard deviation and the second one to the difference with the previous order.

Accuracy	$r_0\Lambda_{\overline{\text{MS}}}$
Next-to-leading	$0.753 \pm 0.022 \pm 0.30$
N <sup>2</sup> LL	$0.619 \pm 0.004 \pm 0.13$
N <sup>3</sup> LL (no PCC)	$0.618 \pm 0.013 \pm 0.0008$
N <sup>3</sup> LL	$0.622 \pm 0.009 \pm 0.003$

estimate. Finally, we mention that there is also an error associated to each of the fit values  $x_i$  coming from the variance of the lattice data points; to obtain this error we consider 1-parameter fits, with  $K_2$  fixed. The error induced in this way in  $\bar{x}$  is much smaller than the other ones we are considering (due to the fact that the lattice points have very small error bars) and can be neglected.

According to the discussion above, our final result for  $r_0\Lambda_{\overline{\text{MS}}}$  reads

$$r_0\Lambda_{\overline{\text{MS}}} = 0.622^{+0.019}_{-0.015}. \quad (6)$$

Our result is compatible with the value  $r_0\Lambda_{\overline{\text{MS}}} = 0.602 \pm 0.048$  given in Ref. [24], which we had been using previously, but has a smaller error. We also mention that a new (preliminary) lattice calculation, which determines  $r_0\Lambda_{\overline{\text{MS}}}$  from the ghost and gluon propagators, obtains a result,  $r_0\Lambda_{\overline{\text{MS}}} = 0.62 \pm 0.01$ , which is similar to ours [26]. We present in Fig. 1(b) a comparison of the static energy with lattice data using the value obtained in Eq. (6) for  $r_0\Lambda_{\overline{\text{MS}}}$ , and the best fit value for  $r_0K_2$  when that value of  $r_0\Lambda_{\overline{\text{MS}}}$  is used, namely  $r_0K_2 = -1.25$ . We note that the error bands due to uncertainties in  $r_0\Lambda_{\overline{\text{MS}}}$  and higher-order terms in Fig. 1(b) are of comparable size.

We would like to emphasize that exactly the same procedure we have described here could be used in the unquenched case. If unquenched lattice data for the static energy at short distances were available we could obtain an unquenched value for  $r_0\Lambda_{\overline{\text{MS}}}$  from it. Combining that result with the value of the strong coupling  $\alpha_s$ , determined from other sources, would provide a determination of the lattice scale  $r_0$ . This determination would be model independent and alternative to other determinations like, for instance, the one using the 1S-2S bottomonium radial excitation energy [27].

In summary, we have updated the comparison of the static energy at N<sup>3</sup>LL accuracy with lattice data by including the recently calculated purely gluonic three-loop contribution to the static potential, which was the last missing ingredient; see Fig. 1. We confirmed that, after canceling the leading renormalon singularity, perturbation theory can accurately reproduce the lattice data at short distances. By taking advantage of this fact, we have obtained a new determination of  $r_0\Lambda_{\overline{\text{MS}}}$ . Our result for the zero-flavor

case is  $r_0\Lambda_{\overline{\text{MS}}} = 0.622^{+0.019}_{-0.015}$ , which improves the precision of the N<sup>2</sup>LL determination (see Table I) by an order of magnitude.

We thank Federico Mescia and Alberto Ramos for useful discussions. The research of X. G. T. was supported by Science and Engineering Research Canada. N. B., J. S. and A. V. acknowledge financial support from the RTN Flavianet MRTN-CT-2006-035482 (EU). N. B. and A. V. acknowledge financial support from the DFG cluster of excellence ‘‘Origin and structure of the universe’’. J. S. also acknowledges financial support from the ECRI HadronPhysics2 (Grant Agreement No. 227431) (EU), the FPA2007-60275/ and FPA2007-66665-C02-01/ MEC grants, the Consolider Ingenio program CPAN CSD2007-00042 (Spain), and the 2009SGR502 CUR grant (Catalonia).

- [1] K. G. Wilson, *Phys. Rev. D* **10**, 2445 (1974).
- [2] W. Fischler, *Nucl. Phys.* **B129**, 157 (1977).
- [3] A. Billoire, *Phys. Lett. B* **92**, 343 (1980).
- [4] M. Peter, *Phys. Rev. Lett.* **78**, 602 (1997).
- [5] M. Peter, *Nucl. Phys.* **B501**, 471 (1997).
- [6] Y. Schröder, *Phys. Lett. B* **447**, 321 (1999).
- [7] T. Appelquist, M. Dine, and I. J. Muzinich, *Phys. Rev. D* **17**, 2074 (1978).
- [8] N. Brambilla, A. Pineda, J. Soto, and A. Vairo, *Phys. Rev. D* **60**, 091502 (1999).
- [9] B. A. Kniehl and A. A. Penin, *Nucl. Phys.* **B563**, 200 (1999).
- [10] A. Pineda and J. Soto, *Nucl. Phys. B, Proc. Suppl.* **64**, 428 (1998).
- [11] N. Brambilla, A. Pineda, J. Soto, and A. Vairo, *Nucl. Phys.* **B566**, 275 (2000).
- [12] A. Pineda and J. Soto, *Phys. Lett. B* **495**, 323 (2000).
- [13] A. V. Smirnov, V. A. Smirnov, and M. Steinhauser, *Phys. Lett. B* **668**, 293 (2008).
- [14] C. Anzai, Y. Kiyo, and Y. Sumino, *Phys. Rev. Lett.* **104**, 112003 (2010).
- [15] A. V. Smirnov, V. A. Smirnov, and M. Steinhauser, *Phys. Rev. Lett.* **104**, 112002 (2010).
- [16] N. Brambilla, X. Garcia i Tormo, J. Soto, and A. Vairo, *Phys. Rev. D* **80**, 034016 (2009).
- [17] N. Brambilla, X. Garcia i Tormo, J. Soto, and A. Vairo, *Phys. Lett. B* **647**, 185 (2007).
- [18] A. Pineda, *J. Phys. G* **29**, 371 (2003).
- [19] Y. Sumino, *Phys. Rev. D* **76**, 114009 (2007).
- [20] M. Beneke, *Phys. Lett. B* **434**, 115 (1998).
- [21] A. Pineda, *J. High Energy Phys.* **06** (2001) 022.
- [22] F. A. Chishtie and V. Elias, *Phys. Lett. B* **521**, 434 (2001).
- [23] S. Necco and R. Sommer, *Nucl. Phys.* **B622**, 328 (2002).
- [24] S. Capitani, M. Lüscher, R. Sommer, and H. Wittig (ALPHA Collaboration), *Nucl. Phys.* **B544**, 669 (1999).
- [25] S. Durr *et al.*, *Phys. Rev. D* **81**, 054507 (2010); A. Ramos (private communication).
- [26] A. Sternbeck, E. M. Ilgenfritz, K. Maltman, M. Müller-Preussker, L. von Smekal, and A. G. Williams, *Proc. Sci., LAT2009* (2009) 210.
- [27] C. T. H. Davies, E. Follana, I. D. Kendall, G. P. Lepage, and C. McNeile (HPQCD Collaboration), *Phys. Rev. D* **81**, 034506 (2010).